

## Article

# Analysis of the Duration of Mandatory Lane Changes for Heavy-Duty Trucks at Interchanges

Min Zhang <sup>1</sup>, Yuhua Nie <sup>1</sup>, Chi Zhang <sup>2,\*</sup>, Bo Wang <sup>2</sup> and Shengyu Xi <sup>2</sup>

<sup>1</sup> School of Transportation Engineering, Chang'An University, Xi'an 710064, China; minzhang@chd.edu.cn (M.Z.); 19907429968@163.com (Y.N.)

<sup>2</sup> School of Highway, School of Highway, Chang'An University, Xi'an 710064, China; wb1010110wb@chd.edu.cn (B.W.); 18955277936@163.com (S.X.)

\* Correspondence: zhangchi@chd.edu.cn

**Abstract:** Due to the different driving characteristics of different vehicle models, inappropriate mandatory lane changes (MLCs) by heavy vehicles at interchanges often lead to serious traffic accidents. Therefore, this paper focuses on the impact of road geometric design on the MLC duration of heavy trucks by using full time-domain trajectory data. Specifically, we use the generalized additive time-varying Cox model to establish the MLC duration model of heavy trucks at interchanges, then analyze the combined influence of geometric elements. The results show that the consistency index of the model is 0.9, indicating that it has advantages in building models in complex environments. The length of the deceleration lane, ramp type, and curve radius have a significant impact on the validity and duration of MLCs. This finding provides a theoretical and methodological reference for the safety analysis of interchange areas and the refinement of road geometric design.

**Keywords:** Cox proportional hazards regression; survival analysis; mandatory lane change; lane changing duration; geometry design

## 1. Introduction

**Citation:** Zhang, M.; Nie, Y.; Zhang, C.; Wang, B.; Xi, S. Analysis of the Duration of Mandatory Lane Changes for Heavy-Duty Trucks at Interchanges. *Sustainability* **2024**, *16*, 6215. <https://doi.org/10.3390/su16146215>

Academic Editor: Marilisa Botte

Received: 7 June 2024

Revised: 3 July 2024

Accepted: 18 July 2024

Published: 20 July 2024



**Copyright:** © 2024 by the authors. Licensee MDPI, Basel, Switzerland. This article is an open access article distributed under the terms and conditions of the Creative Commons Attribution (CC BY) license (<https://creativecommons.org/licenses/by/4.0/>).

Interchange mainline accidents are more frequent than ramp accidents [1], and about 40% of mainline traffic accidents are caused by various types of mandatory lane changes (MLCs). Due to the driver's concern about missing an exit, continuous lane changes and emergency lane changes often occur in front of the interchange diversion area. Continuous lane changing usually involves interruptions in the lane changing process [2], and emergency lane changing, such as the driver starting to change lanes only after approaching the exit, usually involves a drastic change in speed [3]. These are defined as invalid lane changes, which typically expose vehicles to prolonged vehicle interactions and generate traffic oscillations, leading to an increased risk of collision [4]. For heavy-duty trucks, they not only have a high accident rate and mortality rate on interchange sections but also easily lead to regional traffic paralysis and may cause secondary traffic accidents and major safety accidents. This means that highway interchanges pose a serious threat to the safety of heavy trucks while changing lanes and have become a pain point that restricts the improvement of highway safety and the healthy development of freight logistics.

The collision risk of MLCs is essentially caused by the instability of vehicle driving caused by the geometric design [5], and the main characteristic of geometric design factors is their long-term stability. Scholars have studied geometric factors related to MLCs through simulation driving or simulation techniques, such as curve radius and curve bending direction [6], as they affect the psychological workload of drivers when changing lanes to the right. In addition, the geometric design differences of the main upstream and downstream road sections can also affect the driving difficulty for drivers [7]. According to the investigation, if sudden changes in road characteristics violate the driver's

expectations, road accidents tend to be more frequent, which can be described by the consistency index of geometric design [8]. The evaluation method for design consistency can be measured by the difference between continuous operating speed and design speed [7,8], and the degree of coordination with the overall alignment of the highway section can also be quantified by the curve length and slope change rate. Inconsistent designs lead to frequent and rapid deceleration of vehicles, and similar influencing factors include daily traffic flow [9]. However, the existing lane changing analysis is based on simplified rigid body models and assumed trajectories, ignoring the heterogeneity of heavy-duty trucks in terms of vehicle dynamics and driving trajectories. For heavy-duty trucks, the safety of MLCs in interchange areas is not yet clear about which interchange design elements affect the degree of safety and how they affect it, resulting in difficulty in accurately controlling the safety margin of design indicators. In recent years, the density of highway networks has gradually increased, and the complexity of the geometric design between interchanges has also increased. The geometric design of interchange areas not only includes horizontal and vertical lines but also involves functional sections such as transition sections, acceleration and deceleration lanes, and weaving areas. The adjustment of one design element often affects the entire interchange design. Therefore, it is necessary to focus on analyzing the impact of geometric design on the exposure time and validity of heavy-duty truck MLCs and analyzing other design elements from a global safety perspective to further improve the traffic safety of interchange areas.

The existing research is mostly based on simulated driving or simulation techniques or on investigating the influencing factors of lane changing over a certain length of area. The emergence of full time-domain trajectory big data in the digital era provides unprecedented opportunities to solve this problem. Among numerous driving characteristic data collection technologies, the high-precision coordinate positioning data obtained through heavy-duty freight floating vehicles in the full time domain and all road sections has a series of significant advantages. Compared with general data, these data have multiple characteristics, such as full time-domain, large range, and high accuracy, which are conducive to comprehensively and accurately grasping the lane changing characteristics of heavy-duty trucks in day and night environments, various interchanges, and different road sections. In addition, analyzing the MLC behavior of heavy trucks can represent the most adverse effects of behavior during the lane changing process in the interchange diversion area, which will guide the refined design of various elements of interchanges in the existing design guidelines. The survival analysis methods applied in the medical field have also achieved similar goals, such as using the Cox survival analysis to study the influencing factors of survival time after discharge in advanced cancer patients [10]. The Cox proportional risk model is a commonly used survival analysis model used to study time-to-event data. Then, scholars in the field of transportation applied the traditional Cox model to conduct a similar analysis of lane change (LC) duration, used to model the relationship between the duration of LC occurrences and related features. But in the Cox model, it is assumed that the impact of covariates on survival time is linear and does not change over time. However, when there is a nonlinear relationship between covariates and survival time, it can lead to autocorrelation patterns in the residual of the model, affecting the estimation of model parameters and the reliability of confidence intervals [10]. Fortunately, the baseline risk function in the Cox model allows for modeling the survival time of events as a combination function of time and covariates. In addition, a generalized additive model (GAM) can be represented by replacing the linear effects of the predicted variables with the sum of smooth functions. Therefore, combining a GAM with Cox proportional risk models can effectively handle the nonlinear relationship between the geometric design and lane changing survival time. The survey object of this study is the duration of ineffective MLCs before the interchange diversion area. We combine the standard model with the GAM [11]. The GAM can use parameter smoothers to model geometric design covariates as nonlinear functions of mandatory lane change duration (MLCD). At

the same time, time components are added to the model to consider the differences in covariates between day and night [12].

The purpose of this article is to analyze the geometric design impact of MLCD of heavy trucks in the interchange diversion area based on the full time-domain trajectory big data of the interchange area, providing theoretical and methodological references for the fine design of interchanges. The main contributions of this study include the following:

(1) By introducing full time-domain, large-scale, and high-precision trajectory big data, this study explores the differences in MLC characteristics of heavy-duty trucks under different geometric elements of interchanges and day and night conditions. In addition, considering the influence of different combinations of geometric elements on different road sections, the impact mechanism of the geometric elements of interchanges on the exposure time of heavy truck MLCs was elucidated, providing an important theoretical basis for truly reflecting the lateral, dangerous behavior of heavy trucks on various road sections of interchanges.

(2) A duration model for MLCs in interchange areas has been established. On the basis of the standard Cox model, combined with the GAM, time-dependent function, and shared fragility parameters, the nonlinear impact of geometric design on MLCs, time-varying effects, and heterogeneity of driver lane changing are considered separately. This provides a more practical and feasible analysis method for analyzing the safety of interchanges and uses actual operating trajectory modes instead of traditional ideal trajectory radii.

The rest of this article is organized as follows. Section 2 provides a review of the literature, Section 3 proposes our improvement methods, Section 4 introduces data preparation and experimental results, Section 5 discusses the results, and Section 6 presents our conclusions and suggestions for future work.

## 2. Literature Review

### 2.1. The Impact of MLC Duration

MLC is typically conducted to reach a specific (or planned) destination [13,14]. Therefore, compared to free lane changing (FLC), it is greatly influenced by the geometric design of interchanges. For geometric design factors, Yuan [15] investigated the safety effects of weaving length, traffic conditions, and driver characteristics on driver mandatory lane changing behavior through a driving simulator. It was found that higher traffic density increases duration, and longer weaving length often reduces drivers' patience when changing lanes [6]. Based on simulated driving data, Zhou [6] evaluated the impact of sight distance and the geometric shape of highway exit diversion areas on driver performance. The results indicate that the smaller the decision distance of sight value, the more likely collision accidents are to occur. In addition, the driver's driving state on the right circular curve is significantly better than that on the left circular curve, as changing lanes to the right on the left circular curve does not meet the driver's expectations. For spatial location, Gong [16] used traffic flow theories such as the Greenshield model and shock wave analysis to determine the optimal location and corresponding optimal lane change area for early lane change warnings based on the impact of traffic delays. Lee [17] analyzed the impact of three types of exit ramps (direct/semi-direct/circular ramps) on driving performance. Cao [18] modeled the duration distribution of waiting for a safe head time to change lanes as an exponential distribution and determined the best position to provide MLC instructions for autonomous vehicles. Although these studies provide insights into the influence mechanism of the geometric design of MLC behavior at interchanges, these results are mostly based on simulated driving or simulation technology and ignore the lane changing characteristics of different vehicles. In addition, the impact of the combination is not clear, such as the impact of the combination of different geometric elements on MLC risk. Therefore, this paper aims to use the full time-domain trajectory data of heavy trucks to solve these limitations. In addition, the initiation of truck diversion maneuvers is not

affected by lagging/leading vehicles in the target lane [19]. So, in this article, the survival duration of MLCs for heavy-duty trucks does not need to consider the influence of vehicles around individual LCs.

## 2.2. Modeling Method for Lane Changing Duration

Survival analysis has shown that modeling the long-term influencing factors during lane changing has a good effect. The main purpose of survival analysis is to estimate the survival function, which describes the proportion of living individuals in a given time. Li [20] indicates that the duration data of lane change execution follows a Weibull distribution. The results [21] indicate that the generalized gamma distribution and non-parametric methods have a high degree of consistency in estimating survival functions.

The methods for modeling the impact of LC duration mainly include Cox and Accelerated Failure Time (AFT) models, which have different applicability in different scenarios. Feng [22] used the AFT method and found that under perfect communication driving conditions with higher spacing, drivers need more time to complete MLC operations. Ali [23] analyzed various driving performance indicators in MLC races using repeated measures ANOVA and a generalized estimation equation in the form of a linear mixed model. Based on a driving simulator, Shang [24] used the Cox survival analysis to model the duration of MLCs for vehicles on small interval ramps of tunnel interchanges. Jokhio [25] conducted a comprehensive analysis of lane change initiation time using the Kaplan–Meier (K–M) method and the mixed-effects Cox proportional hazards model and identified factors that significantly affect lane change initiation time. Li [20] studied the differences in the influencing factors of LC duration using three accelerated failure time models, and the results showed significant differences in LC characteristics between these two types of vehicles. The Cox model is suitable for investigating variables with long-term effects. The results indicate that the Loglogistic AFT model exhibits more reliable results than other regression models [21]. Ali [1] used a duration model based on parameter AFT danger to establish the minimum gap time between interacting vehicles during MLCs. Dillmann [26] showed that involving drivers in lane changing can improve autonomous driving safety. Ji [27] modeled lane changing events as two interrelated stages of behavior: "stay" and "execute". The parameter estimation results indicate that the driver's decision on phase change is influenced by the surrounding conditions, lane changing purpose, direction, and departure lane. In addition, scholars have provided information on the survival distribution of LCs at different times. The research above shows that the Cox model or AFT model based on the standard can effectively analyze the influencing factors of lane changing duration and provide insights for further improving the safety of lane changing.

However, because the standard Cox model is insufficient in considering the nonlinear influence of covariates, it is necessary to extend the standard model. Zhao [28] used the GAM to explain the nonlinear effect of covariates; Coupe [11] compared the difference between cubic spline and P-spline in linguistic nonlinear modeling. In our study, we can model the covariate as a nonlinear function of the lane change danger duration and consider different nonlinear smoothers for comparison. In addition, the influence of geometric elements on MLCs is different during the day and night. Therefore, some scholars consider this problem by adding time-dependent parameters to the standard model. For example, Zhang [12] used time-varying covariance to estimate the impact of covariates on survival time, and our model can establish each covariate as a function of time variables. Due to the heterogeneity of drivers' lane changing, it is necessary to use shared fragility in the model for correction. Ben [29] used the Cox pH regression model to model the survival rate of CHF patients, which showed that the shared fragility correction improved the performance of the basic Cox pH model. The most common alternative to the Cox model is the AFT model, which assumes that the explanatory variable (or covariate) has a multiplicative effect on survival time, manifested as accelerating or slowing down the process from time to event. Madhiah [30] conducted a model comparison and found that, compared to the Cox model, AFT showed better survival outcomes under the lowest

Akaike information standard and best fit conditions. However, for complex interchange geometric designs, modeling the lane changing survival time of heavy trucks as a fixed distribution using the AFT method may not truly reflect the MLC characteristics of heavy trucks in specific areas. Considering these limitations, we improved the standard Cox model and tested it using a full time-domain trajectory set of heavy-duty trucks.

### 3. Methods

Our method steps are shown in Figure 1. First, heavy truck trajectory data were collected from 38 interchange areas, which included more than 50 attributes per driver. Then, the data were cleaned and matched with the map to obtain MLC sequences, and the feature selection was carried out through the SHapley Additive exPlanations (SHAP) algorithm. The final data set included 18 variables for each record. Then, the GAM was used to nonlinearize the characteristics, and the time-dependent module was introduced to consider the circadian conditions, as well as the shared fragility to modify the model to obtain the relative risk value of geometric characteristics. Finally, compared with the guidelines of interchange, suggestions for design improvement were put forward.

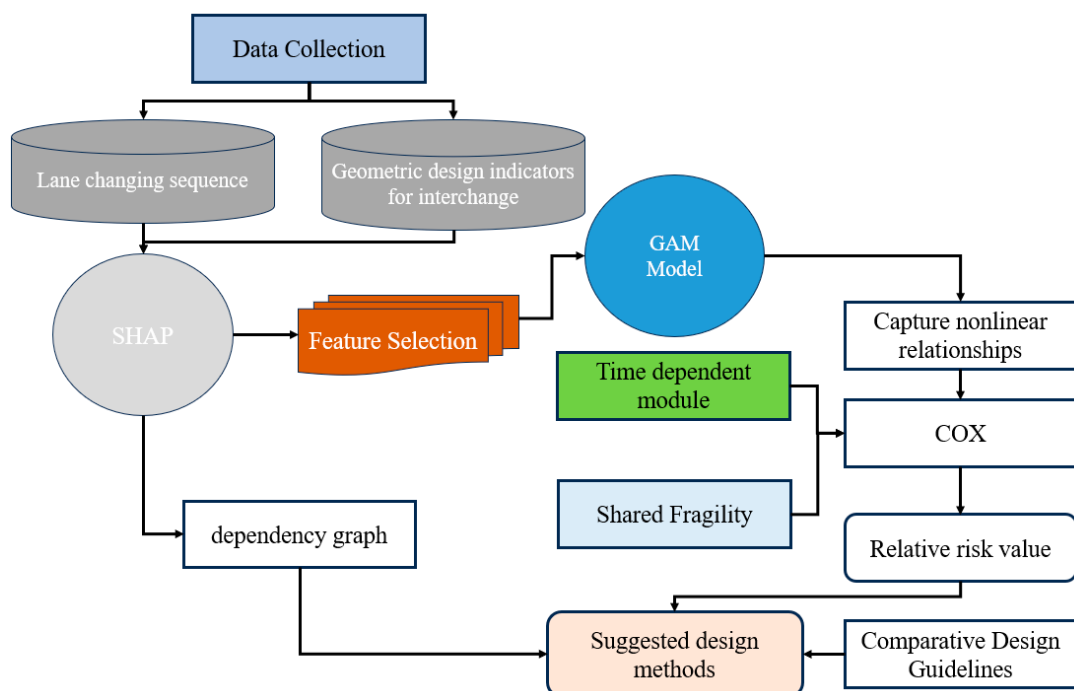


**Figure 1.** Research steps and analysis process.

#### 3.1. Feature Selection

The SHAP model is commonly used to explain the importance of complex model features, such as deep-learning models [10]. Due to its powerful parsing and visualization capabilities, some scholars have gradually applied it to traffic safety research in recent years. The calculation of SHAP values is based on iterating the combinations of all possible feature subsets, thus comprehensively considering the impact of each feature under different combinations.

In this study, we used the Scikit Learn Wrapper interface provided by XGBoost (version 1.4.0) to train a random forest model and selected features based on two target variables (MLCD and MLC validity). Then, the SHAP library in Python (version 3.9.5) generated SHAP values for each sample. The SHAP value represents the degree to which each feature affects the model output. The SHAP value is displayed in the decision graph, which provides a detailed view of the internal workings of the model and demonstrates a large number of feature effects that are clearly visualized through multi output prediction

[31]. This process used 30 features, ranked in descending order of their impact on the model. A total of 18 features were rated as having the greatest impact by both algorithms and were therefore selected for survival analysis. Finally, we used Pearson correlation coefficient to test the correlation between these variables and discarded three highly correlated variables, as shown in Table 1. Therefore, this method identifies the variables for survival analysis modeling.

**Table 1.** Features selected by SHAP.

Dimension	Characteristic Symbol	Implication	Dimension	Characteristic Symbol	Implication
Time-varying environment	$x_1$ (mm/h)	Average rainfall per hour during LC time	$x_5$ (m/s)	$x_6$ (1\2\3)	Geometric design consistency: the difference between road section design speed and operating speed
	$x_7$ (veh/h)	Hourly traffic volume			The bending direction of the road curve in the influence area (outside/straight/inside)
Spatial position	$x_{13}$ (0 or 1)	Day or night	$x_8$ (1\2\3)	$x_9$ (m)	Direct ramp, semi-direct ramp, ring ramp
	$x_2$ (m)	The length from the diversion nose end			Curve radius
Lane changing state	$x_3$ ( $\text{m/s}^2$ )	Acceleration before LC	Road geometry design	$x_{10}$ (m)	Gradient section length
	$x_4$ (m/s)	Speed before LC		$x_{11}$ (m)	Deceleration lane length
Analyze variables	$y_1$ (s)	event time	$x_{12}$	$x_{14}$ (1\2\3)	Number of deceleration lanes
	$y_2$ (1 or 0)	Occurrence			The bending direction of the road curve outside the influence area (outside/straight/inside)
				$x_{15}$ (m)	Distance between dividing and merging nose ends

### 3.2. Generalized Additive Models (GAMs)

With the emergence of nonlinear effects in covariates, linear regression models cannot give promising results, so it is necessary to introduce nonlinear descriptions, such as GAM, which enables us to fit the model with nonlinear smoothers without specifying specific shapes in advance. GAM solves this difficulty by allowing smoothing functions or smoothers in the linear prediction components of the regression model, as well as “unsmoothed” covariates. Therefore, the general equation of GAM can be written as:

$$g(E(Y)) = I + s_1(x_1) + \dots + s_n(x_n) + \varepsilon, \quad (1)$$

where  $x_1 \dots x_n$  is the predictor,  $s_1(x_1), \dots, s_n(x_n)$  is the smoothing term associated with these predictors,  $I$  is the intercept,  $\varepsilon$  is the residual error term,  $Y$  is the dependent variable,  $E(Y)$  is the expected value, and  $g$  is the link function.

The smoothing term selects a parameter smoother, such as a multinomial, a fraction multinomial, a piecewise multinomial, or a B-sample. The penalty smoother is used to find the best value for the smoothing parameter, which controls the amount of smoothing, that is, how well the smoothing term fits the original predictor. The geometric design variables of the overpass area are fitted to the nonlinear function of the research target using the GAM method.

### 3.3. Survival Analysis

Survival analysis is widely used in the medical field to determine the factors influencing the survival time of cancer patients [30]. In recent years, its analysis method has been used to analyze the survival period of lane changing. It can be used to estimate the end time of lane changing and the most relevant factors to risk in lane changing when the vehicle begins to shift lanes.

According to the concept of survival analysis, the elements of MLCD for truck survival analysis are defined as follows:

(1) Event and event duration: The starting point of the event is the moment when the vehicle begins to deviate from the lane. The endpoint is the moment when the lane changes to the target lane and returns to the positive direction. The time difference between the starting and ending points of an event is the duration of the event.

(2) Event result: Event result indicates whether the MLCs of vehicles on the exit ramp are effective. When the vehicle is unable to complete a lane change in the designated area,  $E = 1$ ; otherwise,  $E = 0$ .

#### 3.3.1. Risk Models in Survival Analysis

The survival function  $y = S(t, E)$  defines the survival outcome, where  $t$  is the time when the event occurred or was reviewed and  $e$  represents whether the event occurred (yes/no). Therefore, the survival function indicates how much time will pass before event  $E$  occurs. The formal survival function is given by the following equation:

$$S(t) = P(T > t), \quad (2)$$

The equation is the probability that the survival time  $T$  exceeds the time  $t$ . The danger function  $h$  represents the probability that the driver who is making a LC at time  $t$  will end the lane change before “ $t + \Delta t$ ”. The danger function is given by:

$$h(t) = P(T < t + \delta | T > t) \quad t \geq 0, \quad (3)$$

A similar question of interest is the relative risk (hazard ratio ( $HR$ )) between LCs obtained by calculating proportional risk.

$$HR = \frac{Hazard(E = 1)}{Hazard(E = 0)}, \quad (4)$$

Provided the hazards of LC exposed to risk factor ( $E = 1$ ) compared to LC not exposed to risk factor ( $E = 0$ ) are not equal.

#### 3.3.2. Time-Varying Cox Proportional Risk Model (T-Cox-PH)

Cox-PH regression determined the relationship between the risk function and the predictor, but Cox believes that the relationship between the risk function and the predictor is linear, which means that variables have a constant impact over time. Since violating this assumption may compromise the effectiveness of the model, we modeled the time-varying effects through interactions with time to compensate for the shortcomings of the standard Cox model.

We used the Time-Varying Cox Proportional Risk model to estimate the geometric impact of covariates on the validity of LC after lane departure. LC that is invalid during this period is considered the subject of review. We estimated the danger function  $h_{i,j}(t, X)$ , which measures the probability of driver  $i$  ending a lane change after the time  $t$  measured from MLC $j$ , as follows:

$$h_{i,j}(t, X_{i,j}) = h_0(t) e^{f_1(x_{1ij}\beta_1) + f_2(x_{2ij}(\beta_2 + \beta_3 g(t))) + \dots}, \quad (5)$$

Among them,  $t$  is the time when the exit ramp lane deviates,  $h_0(t)$  is the unique baseline risk for all drivers in the LC library, and  $f(k)$  is a function of the GAM that converts covariates into nonlinear relationships.  $g(t)$  is used to introduce some variables into time effects. It is assumed that the influence of  $x_1$  is constant, while the influence of  $x_2$

allows for variation with a certain function of the analysis time. If the model is a discrete duration model, such as a time-dependent Logit or Probit model, non-proportional hazards can be constructed through similar interactions with time.

### 3.3.3. Shared Frailty of Cox-PH

The frailty model is an extension of the Cox-PH model, in which potential heterogeneity is included as the random multiplication effect known as fragility. In our study, frailty corresponds to repeated LCs by the same driver. These LCs are grouped, and the observed results may be correlated within a group. This correlation is believed to be caused by potential covariates or omitted covariates (“frailty”) that are common when the same driver is admitted to the hospital. These potential covariates trigger an unobserved heterogeneity.

We focus on multivariate shared frailty model. The multivariate frailty model extends the Cox-PH model by multiplying it by the baseline hazard function  $h_0(t)$ , so that the risk of LC also depends on the potential random variable, namely the frailty random variable  $Z_i$ . Different frailty distributions represent different ways of expressing unobserved heterogeneity and affect observed covariates in different ways. Therefore, the weak distribution will reduce or increase the risk for each driver, depending on  $Z_i < 1$  or  $Z_i > 1$ . The weak danger function  $h_{ij}(t, Z_i, X_{ij})$  of driver  $i$ 's  $j$ th LC is represented as:

$$h_{ij}(t|Z_i, X_{ij}) = Z_i h_0(t) \exp(\alpha^T X_{ij}), \quad (6)$$

Over time, the fragility value remains constant and is shared among each driver's LCs. Therefore, assuming the sub-condition, it is assumed that the survival duration of the driver  $i$ 's LC is independent [32]. For driver  $i$  of LC $j$ , the conversion between the hazard function  $h_{ij}$  and survival function  $S_{ij}$  at the driver's level is given by the following equation:

$$S_{ij}(t|Z_i, \alpha, X_{ij}) = \exp(-Z_i \int_0^t h_0(s) ds \cdot \exp(\alpha^T X_{ij})), \quad (7)$$

The survival function  $S$  of the total driver is given by the following equation:

$$S(t|Z, \alpha, X) = \exp(-Z \int_0^t h_0(s) ds \cdot \exp(\alpha^T X)), \quad (8)$$

We tested two distributions of the frailty random variable  $Z$ —with a mean of 1 and a variance of  $\theta$  unknown gamma and Gaussian distributions. We reported the results of the Gaussian distribution and indicated that these results are very similar to those obtained using the gamma distribution. We used the penalty partial likelihood method running on the R “survival” and lifeline packages in Python to estimate the shared frailty model [29].

## 4. Experiment Results

### 4.1. Data Preparation

The data in this article are the floating vehicle trajectory data of heavy vehicles, collected from 1 June 2023 to 1 September 2023, with a sampling frequency of 1 Hz, positioning accuracy  $< 1$  m, and speed measurement accuracy of 0.2 m/s. The trajectory covers over 140 km of highways and is obtained by the onboard GPS of heavy trucks. As shown in Figure 2a, our data include basic information such as longitude and latitude, vehicle ID, vehicle speed, heading angle, etc. The positions of these trajectories can match the road geometry design data, weather, accidents, and traffic volume information provided by the road section management company. Compared to the HighD [21] and NGSIM [33] datasets, the floating vehicle trajectory data cover a longer road segment, have a complete time range, and come with rich spatial information. This provides the possibility to study the impact of different spatial position attributes on the trajectory, which is the advantage of our data. As shown in Figure 2b, our data include complex forms of interchanges, covering 38 interchanges (68 exit ramps) (only a few are listed). In addition, we use the “Pyautocad” library in Python to display all trajectories on CAD maps and then import them into Ovi Maps. As shown in Figure 2d, each interchange was passed by an average of

10000 different heavy trucks within a month, and we used data from a total of 3 months. Finally, we use map matching technology to divide the trajectory into different paths as shown in Figure 2c.

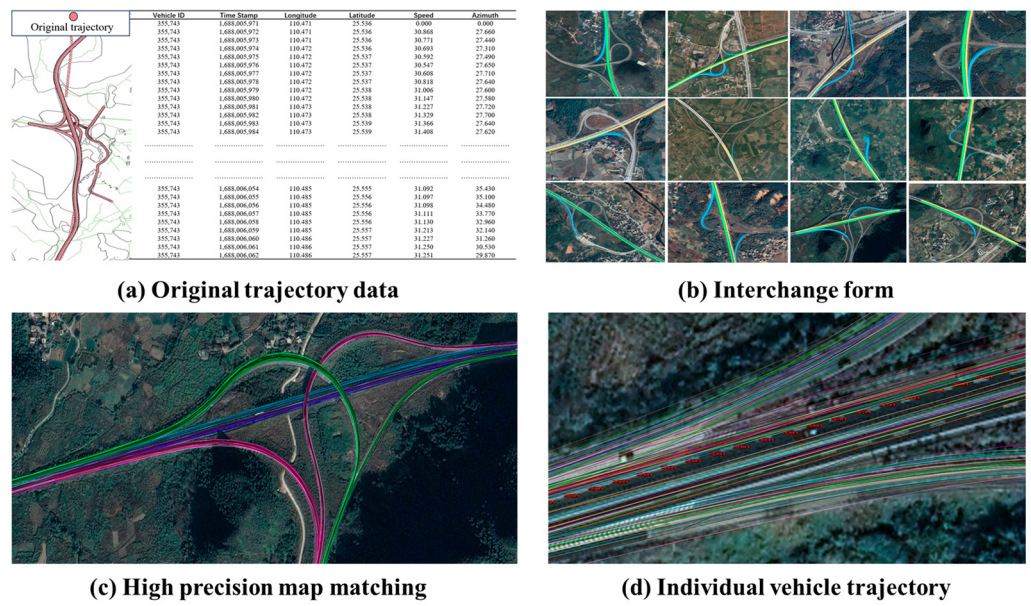


**Figure 2.** Visualization of mandatory lane changing trajectories in interchange and diversion areas. The blue line in Figure 2b represents the trajectory of the diversion, while the other colors represent the trajectories passed through.

As shown in Figure 3, the geometric elements in front of each interchange diversion area include the mainline section, gradient section, deceleration lane section, and solid line section (where lane changing is prohibited). In addition, based on the data of the road centerline, a road center stake system is established every 10 m. The purpose of establishing a pile system is to determine the lane changes of vehicles and their lateral positions relative to the road centerline and convert these points into a Frenet coordinate system with the road centerline as the reference line. To minimize lane change (LC) recognition errors, we have established multiple rules for LC detection, as shown below:

Step 1: Calculate the lateral offset of the continuous trajectory from the road centerline per second. Defines that the outward offset is negative, and the inward offset is positive.

Step 2: Sum the lateral continuous offsets and extract the travel data of these trajectories when the cumulative lateral deviation exceeds the width of the vehicle.

Step 3: For travel processes in Step 2 where the cumulative lateral offset reaches the vehicle's width, determine the lane number at the starting point and the lane number at the ending point. If these two lane numbers are different, classify it as a lane change (LC).

Step 4: For the collected LC data, the right lane change of vehicles approaching the exit ramp before passing through the exit ramp sign and before the diversion nose is defined as a mandatory lane change.

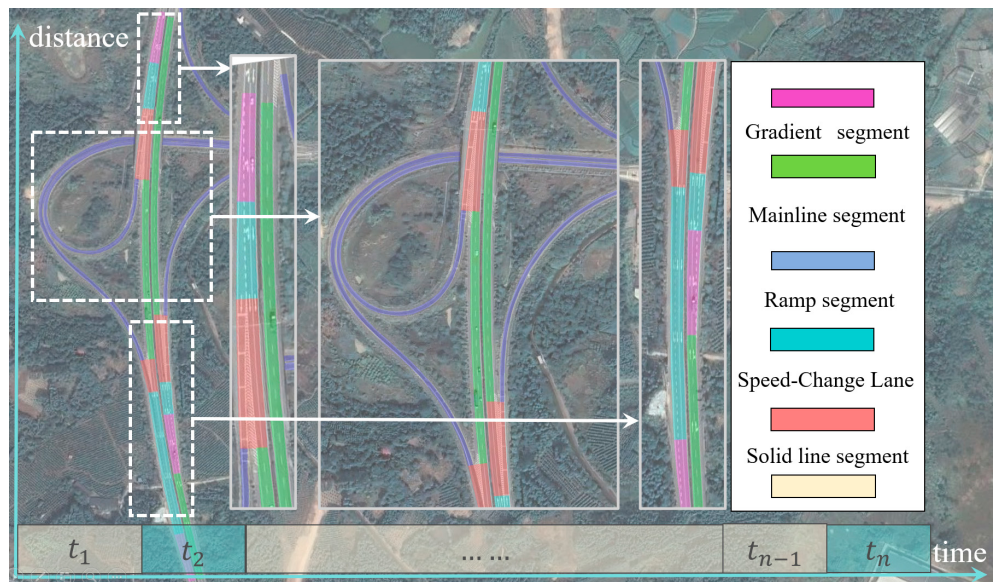


**Figure 3.** Schematic diagram of spatiotemporal slicing in the interchange area.

As shown in Figure 4, we present an example of extracting the forced lane change behavior in front of the interchange diversion area. This figure contains the complete trajectory of the floating truck in the diversion area and the lane change offset sequence extracted through rules. Each region displays the frequency of the starting position of lane change through a heatmap. Through this method, the lane changing trajectories of all interchanges can be extracted.

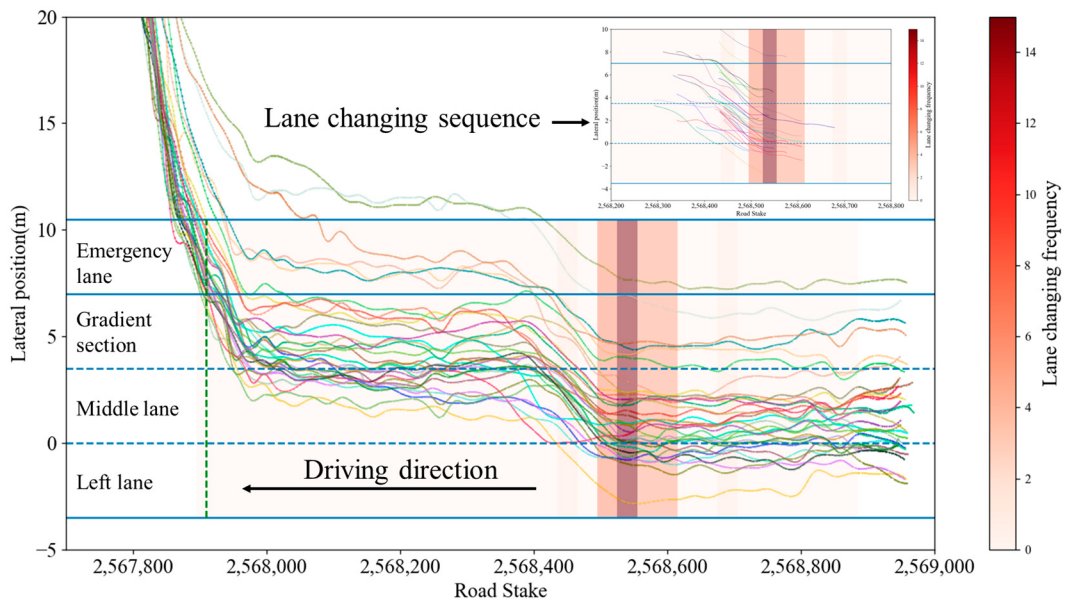


**Figure 4.** Lane changing extraction and frequency distribution in interchange areas.

#### 4.2. Descriptive Statistics

This study extracted a total of 5845 cases of mandatory and FLC of heavy-duty trucks in different interchange diversion areas. Considering the differences in left and right lane changing types [34], this study focuses on comparing the duration of free right lane changing and mandatory lane changing. Figure 5 shows that the duration of MLCs for heavy-duty trucks is 0.5~1 s shorter than FLC, and the coefficient of variation for MLCD is higher. From the location of LC, Figure 6a shows that the MLC in front of the interchange diversion area is mainly distributed around 170 m~800 m. Figure 6b shows that the invalid lane

change duration is concentrated at 5 s, which is about 3 s longer than the valid MLCD. In addition, compared to the MLCD of small cars that have been studied [24], the MLCD of the heavy-duty trucks is about 0.6 s longer than small cars.

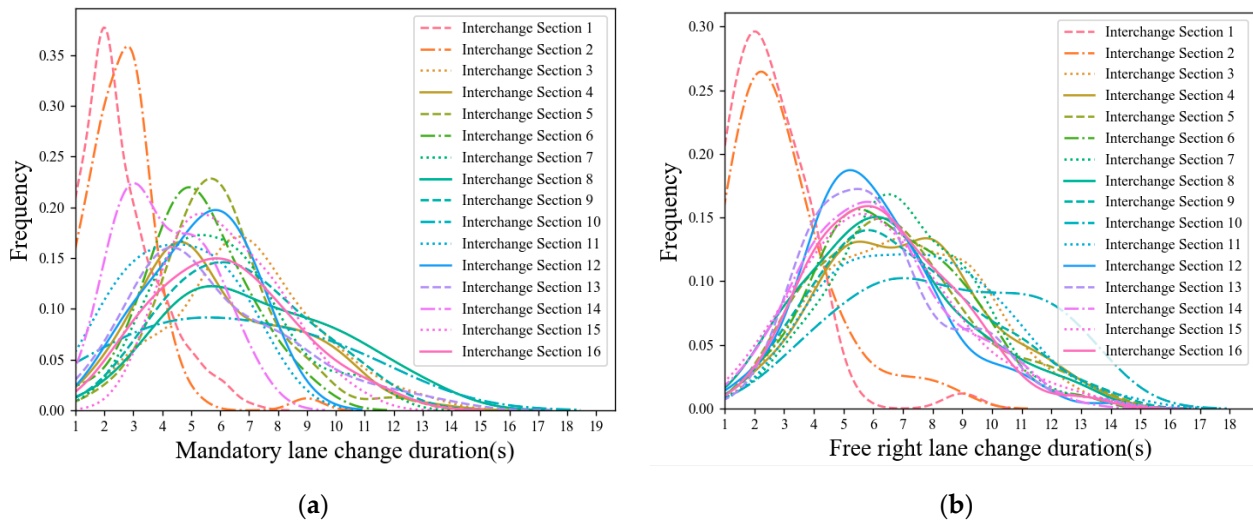


**Figure 5.** Lane changing duration distribution. (a) MLC. (b) FLC.

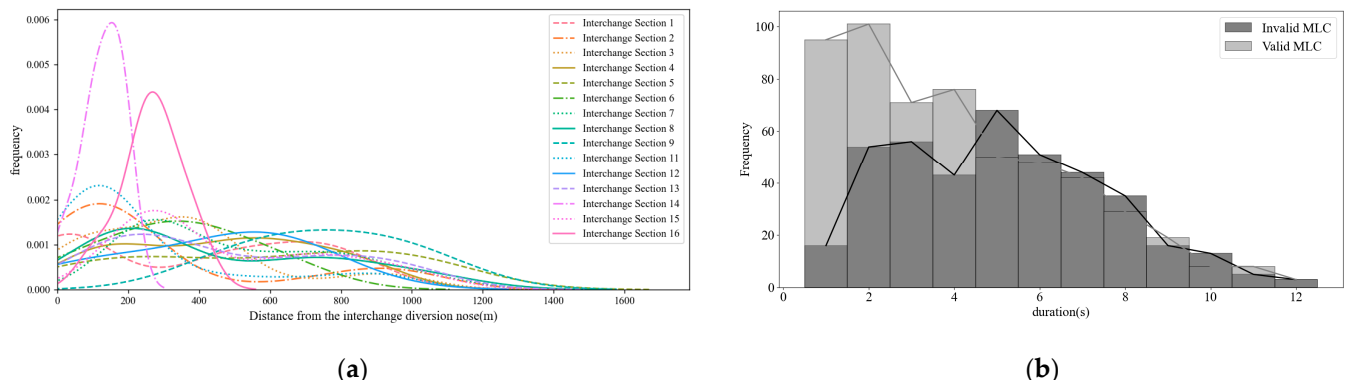


**Figure 6.** (a) Distribution of lane changing positions for different interchanges. (b) Comparison of valid and invalid lane changing duration.

#### 4.3. Feature Selection

Figure 7a,c show the SHAP summary of the duration and validity of MLCs, respectively. The results in the figures indicate the importance of the variables. Figure 7b,d represent decision graphs. In the “decision\_plot” function of the SHAP library, the link parameter is used to specify the link function to be displayed. The LC duration uses the “identity” link function, and the MLC validity uses the “logit” binary classification function. Specifically, each horizontal line in the decision graph represents the influence of a feature. The position of the line represents the impact of a given feature value on the model output. If the line is biased to the left, it indicates that the feature value has a negative impact on the output of the model; if the line is biased to the right, it indicates a positive impact. In addition, decision graphs can intuitively display the explanatory information of individual samples or predictions. By observing decision graphs, it can be understood that the model is based on nonlinear relationships of various features. Firstly, consider the impact of MLCD, where the acceleration before changing lanes in the vehicle’s own state dimension has the greatest impact on the duration. The consistency of geometric design dimensions has a secondary impact on geometric design consistency; the spatial location dimension and external environmental traffic flow are significant influencing factors. In addition, speed, curve direction, and radius also have a significant impact, while others

have a weaker impact. Secondly, considering the impact of MLCs' valid ratio, spatial location plays a decisive role. That is to say, the closer the vehicle is to the diversion nose when a MLC has not yet been carried out, the greater the probability of an invalid MLC occurring. In addition, the geometric inconsistency of geometric design dimensions and the length of deceleration lanes are significant factors affecting the validity of MLCs, while all other factors have a relatively small impact. The nonlinear relationship and feature importance that affect MLC behavior were demonstrated through decision graphs and summary graphs, respectively, in order to select covariates from a large number of features, as shown in Table 1.

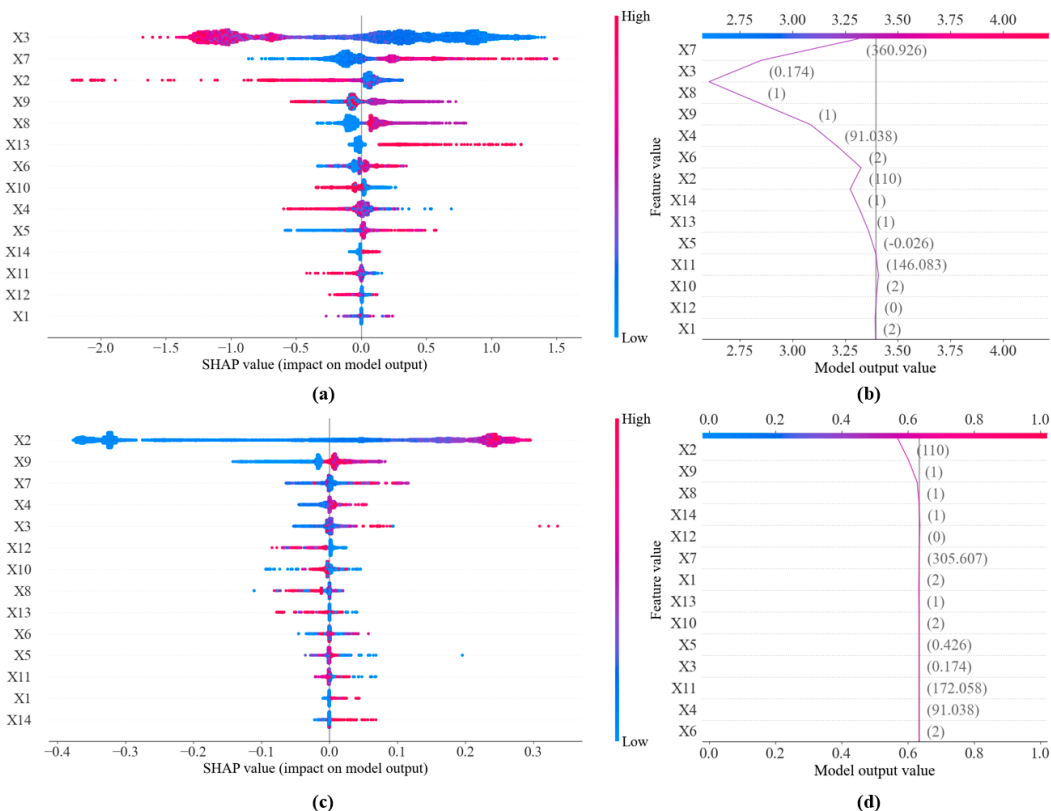


**Figure 7.** (a) SHAP summary of MLCD. (b) SHAP decision graph for MLCD. (c) Summary diagram of MLC valid probability. (d) Decision graph for MLC valid probability. The order of variable codes in the figure corresponds to Table 1.

In order to analyze the key influencing factors of MLCs in heavy-duty trucks, after selecting features, we used the Kaplan–Meier non-parametric survival analysis to establish their survival and hazard functions and quantitatively analyzed the distribution characteristics of MLCs under a certain influencing factor (Figure 8). As shown in the figure, the x-axis represents the duration of lane changing in seconds, and the y-axis represents the cumulative probability curve of MLCs ending within time  $t$ . The survival probability at the beginning (0 s) is 1.0, indicating that the lane is starting to shift. However, as time increases, the probability of survival decreases, indicating an increase in the number of events ending (the end of lane changes). Figure 8i shows that the survival function rapidly decreases within the first 4 s. A sharp decline means that most MLCs are completed in a short period of time. In fact, this period accounted for almost 80% of the total lane change cases. After 8 s, the probability gradually decreases, indicating that over time, MLCs are still surviving less and less. About 20% of lane changes are still active after 8 s, and only 8% of lane changes last for more than 10 s.

The Kaplan–Meier (K–M) method is a statistical method used to estimate the probability of an event occurring within a given time period. We compared different groups by

calculating the survival rate at each time point through a curve, as shown in Figure 8. The survival duration of FLCs is longer than that of MLCs, indicating that MLCs are more urgent and aggressive, while invalid lane changes last longer than valid LCs, indicating that invalid lane changes are exposed to danger for a longer period of time. Figure 8a shows that the inner side of the curve increases the duration of a LC, but there is no significant difference between the outer side of the curve and the straight line. Compared to direct ramps, semi-direct ramps will increase the LC duration, as shown in Figure 8b, and the LC duration under circular ramps is the longest, exacerbating the risk. Figure 8c shows that a small radius can also improve MLCD; for the length of the gradient section, Figure 8d indicates that an increase in its length will increase the duration, while a decrease in the length of the deceleration lane will exacerbate the unsafe increase in duration, as shown in Figure 8e. The dual-lane ramp will increase the duration (Figure 8f). Figure 8g indicates that an increase in the distance between the merging and diverging nose ends of different interchanges will also increase the MLCD. Figure 8h shows the effect of the curve direction within the range of 0–800 m before the diversion zone on MLCD, similar to the results in Figure 8a. Through K-M analysis, it can be found that, for some geometric design indicators, such as the length of the deceleration lane changing within a certain range, it will not have a significant impact on the MLCD. Therefore, it is necessary to apply non-linear techniques to the extension of the MLC risk function.

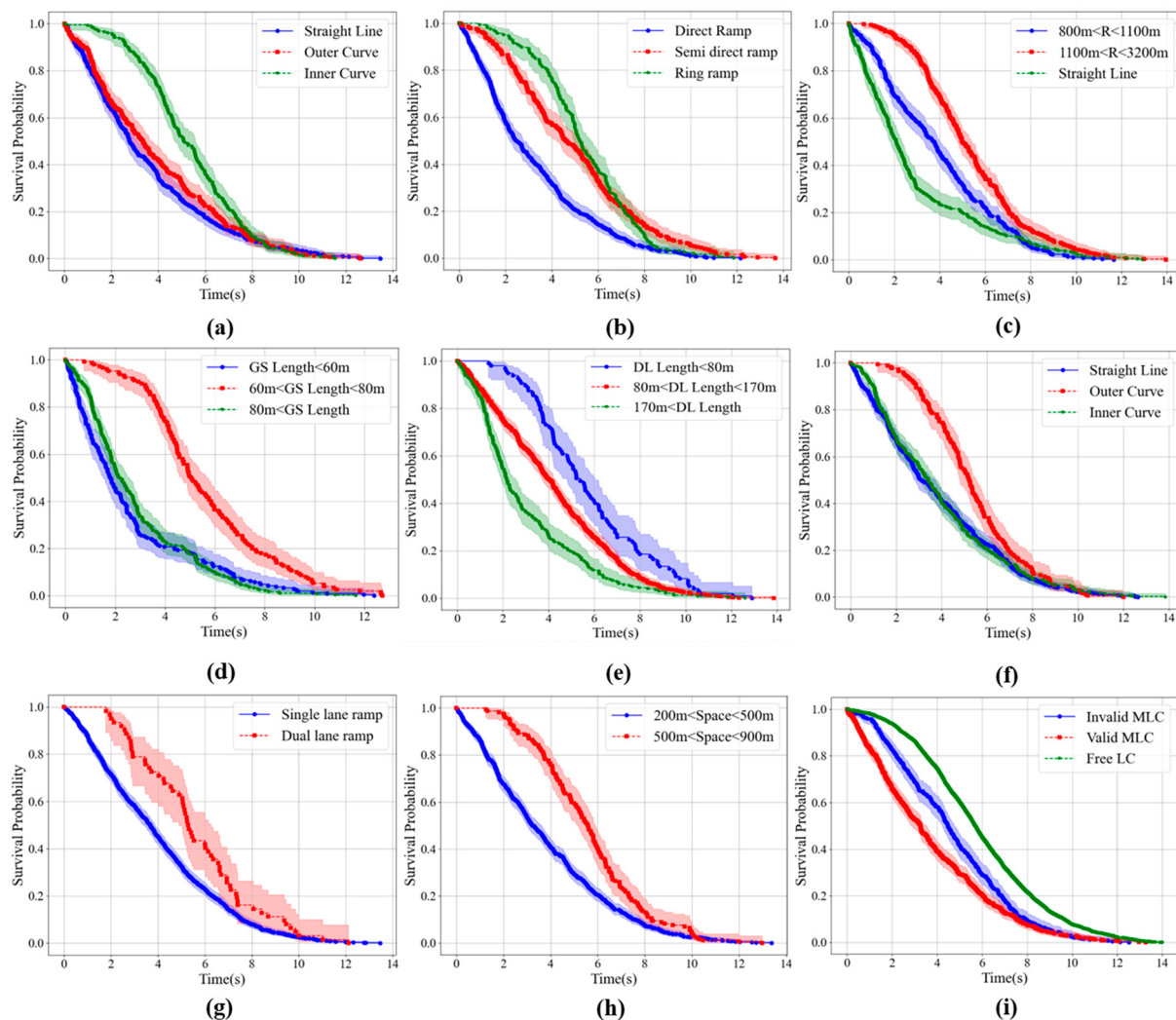


**Figure 8.** K-M analysis of individual influencing factors on MLCD. (a) The bending direction of the road curve outside the influence area. (b) Ramp type. (c) Curvature radius. (d) Gradient section length. (e) Deceleration lane length. (f) The bending direction of the road curve inside the influence

area. (g) Number of ramp lanes. (h) Distance between dividing and merging nose ends. (i) The validity of MLC.

#### 4.4. Feature Nonlinear Modeling

The standard Cox model considered has shortcomings in considering the nonlinear relationships of geometric design elements. By using GAM technology, MLC events are established as nonlinear functions of covariates (Figure 9). Therefore, it is necessary to consider the smoothing term in the proportional risk model, and we have considered an anti-Gaussian GAM with a smoother. Finding the most suitable smoother requires comparing different options and models with Akaike Information Criterion (AIC) and Bayesian Information Criterion (BIC) measures. It is usually recommended to automatically estimate the smoothing parameters [28], that is, try the penalty version of the smoother. We compared three commonly used smoothers: cubic spline, P-spline, and B-spline. Regarding cubic splines, the penalty has been modified to shrink towards zero when the smoothing parameter becomes infinite. Specifically, this means that no relationship is correctly identified, i.e., with 0 effective degrees of freedom, rather than modeling with one degree of freedom as in standard cubic splines. For P- and B-splines, the second-order difference of coefficients is penalized to control the smoothness of the spline.

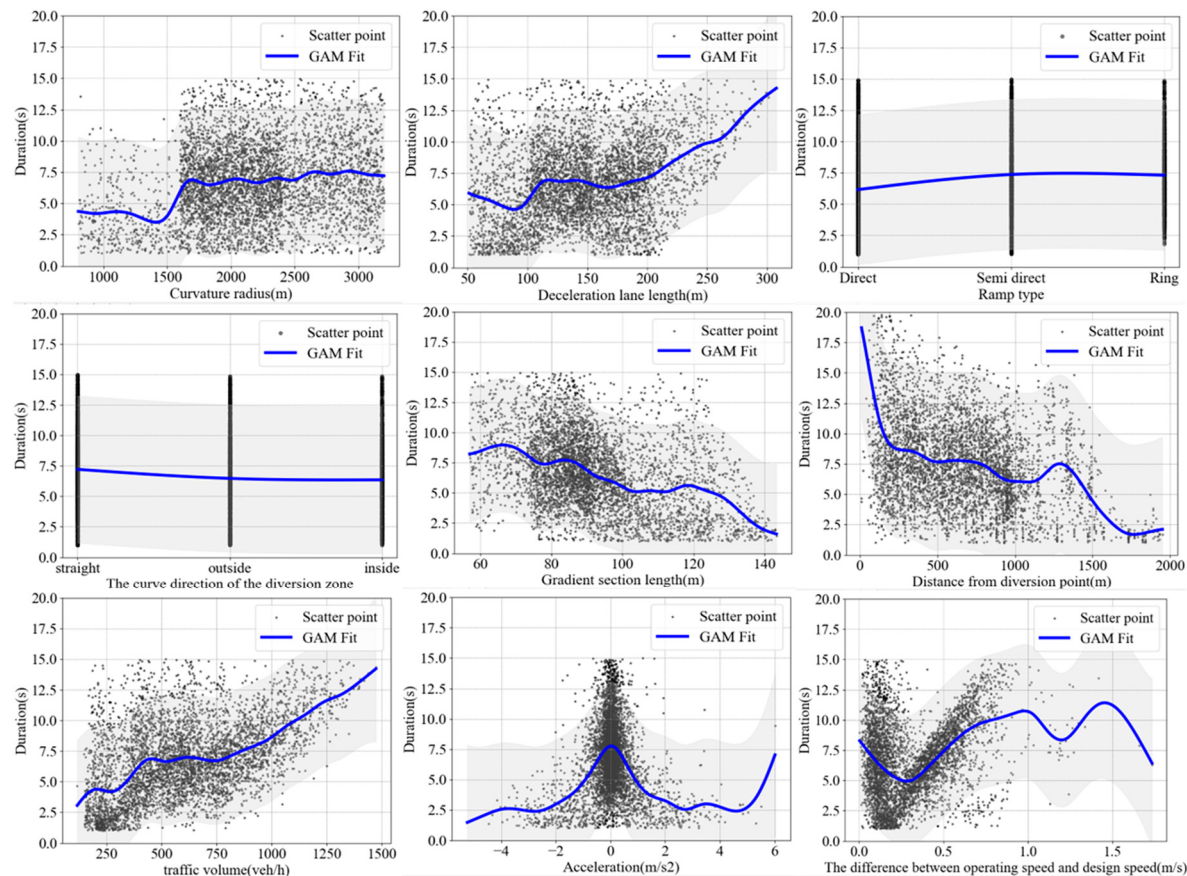


**Figure 9.** Fitting the relationship between response variables and covariates using GAM smoother.

Different smoothing functions lead to different optimizations. Overall, although P-splines and B-splines allow for a direct penalty on coefficients, the cubic spline model has the lowest AIC and BIC, so it should theoretically be preferred, although it does not provide any simple explanation for the shape of nonlinear relationships, such as MLCD and curvature radius.

Although the cubic spline model performs better in metrics, sometimes this highly flexible model does not intuitively reflect the true structure of the data. For example, a cubic

spline model is used to model the nonlinear relationship between factors such as vehicle speed and headway and lane changing time. However, in reality, certain parts exhibit sharp changes within a specific range, so it is necessary to balance and consider other smoothers. In addition, for the estimation of smoothing parameters, using automatic estimation is usually a good choice because it can use the features of specific datasets to calibrate the model, reducing subjective bias and improving the model's generalization ability.

#### 4.5. Model Results

Through K-M non-parametric estimation, it was verified that 2 out of 18 features slightly violated the proportional risk assumption, acceleration and velocity, which are due to the influence of velocity over time, while the remaining variables conform to the assumption. We also used Cox.zph (functional functions) from the survival package in R to examine the hypothesis of Cox models with shared fragility, as shown in Table 2, and all *p*-values, except those at night, were less than 0.06, indicating overall compliance with the PH hypothesis.

**Table 2.** Variables that meet significance levels in the Cox-PH shared frailty model.

Covariate	Se(coef)	<i>p</i> -Value	-Log2( <i>p</i> )
$x_2$	0.00	0.00	144.75
$x_3$	0.05	0.00	31.61
$x_5$	0.24	0.00	11.64
$x_6$	0.11	0.00	13.91
$x_7$	0.00	0.00	16.83
$x_8$	0.10	0.00	45.63
$x_9$	0.12	0.00	16.06
$x_{11}$	0.13	0.00	79.09
$x_{12}$	0.34	0.00	30.93
$x_{13}$	0.12	0.06	3.97

In the summary of the Cox Time-Varying Fitter model, the standard error of the covariate coefficients (Table 2) characterizes how the impact of variables on risk rates changes over time and emphasizes when these effects are significant. Our model is divided into day and night. Specifically, the standard errors of the coefficients for the impact of the number of deceleration lanes and geometric design consistency index on the duration of lane changing are 0.34 and 0.24, respectively, indicating that they have a greater impact on the danger time of MLCs at night. In addition, the standard errors of spatial position, acceleration, and traffic volume are relatively small, all less than 0.1, indicating that the impact of these covariates is constant at different time periods.

The relative impact of factors affecting MLC validity estimated by the Cox-PH regression is shown in Table 3. Next, we use a shared fragility multiplier with a gamma distribution to correct the Cox PH model. As shown in Table 3, shared fragility explains the changes in data, while fixed effects cannot explain these changes. Adding shared fragility to drivers can enable each driver to have a different baseline hazard rate, rather than assuming that all drivers share the same baseline hazard level. The distribution of random effects is assumed to be gamma, with an average value of zero. The regression coefficients of the Cox model can explain the risk impact of individual factors on MLCs. Taking X2 as an example, the regression coefficient is 0.001 and the relative risk is 1.001, indicating that when the decision line of sight is reduced by 100 m, the risk rate at the end of the lane change increases by 10%.

However, the risk coefficients above represent an overall level of impact. To further explain the interaction between covariates, it is necessary to add the SHAP's dependency graph for analysis. As shown in Figure 10a, when a driver changes lanes at a distance of 1000 m from the diversion zone, changing lanes at a stable acceleration can reduce the

risk, but when a driver changes lanes 500 m away from the diversion area, adopting a fast LC strategy can reduce the risk. Figure 10b,c,e show that the consistency index of operating speed, the direction of curve curvature, and the type of ramp have significant differences in the impact on MLC under different traffic volumes. The impact of ramp type on MLCs is attributed to vehicles traveling on semi-direct and circular ramps slowing down at the front of the ramp, especially on circular ramps. As traffic volume increases, this will increase the workload of drivers to varying degrees. The regulations on the length of deceleration lanes in the “Design Guidelines for Interchanges in China” are related to the design speed. However, the results in Figure 10d indicate that it is also related to the bending direction of the circular curve. In addition, we also conducted a statistical analysis on the relationship between the number of traffic accidents at each interchange within 3 years and the average MLCD. As shown in Figure 11, this relationship shows a concave curve, with fewer accidents occurring within an average lane changing time of 5 s. However, the growth rate of accidents sharply increased after 5 s, indicating that the longer the exposure time for lane changing, the more likely it is to lead to accidents, which is consistent with the existing research [21]. These results indicate that the geometric elements of interchanges have a significant impact on MLCs, and these analyses emphasize that the geometric design of interchanges should not only consider the impact on the speed of small vehicles, but also the lane changing behavior of heavy trucks, as MLCs have caused a significant proportion of serious traffic accidents.

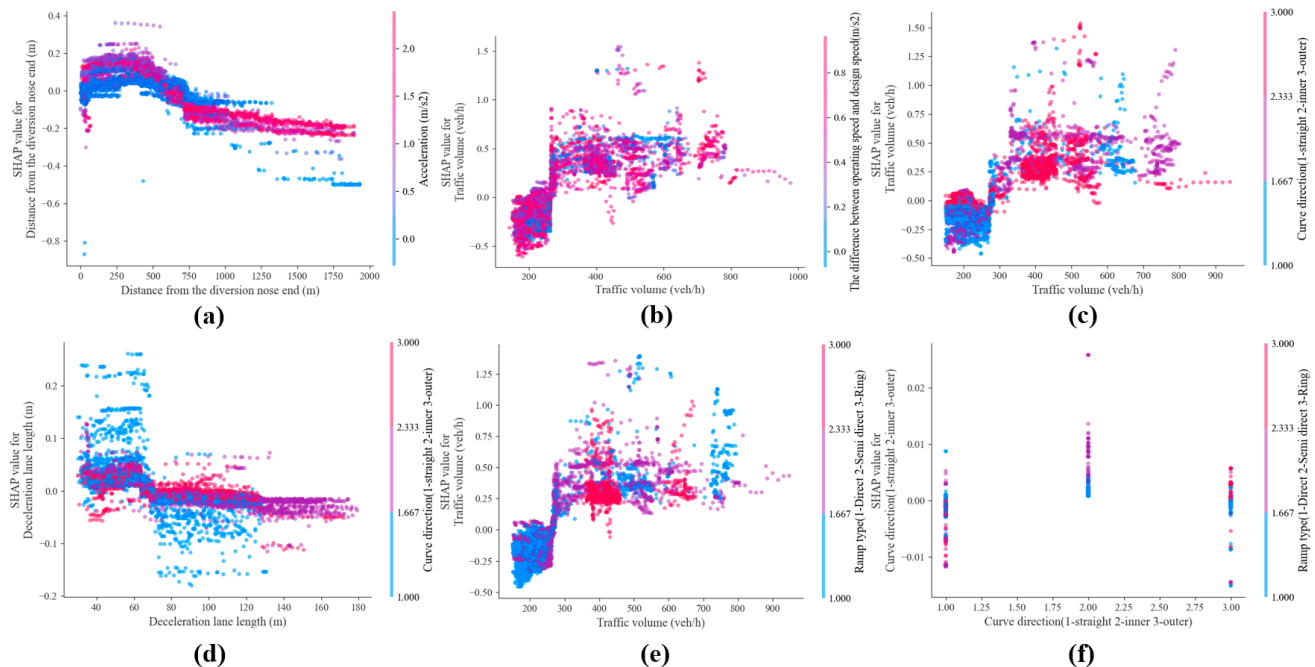


**Figure 10.** Dependency graph of SHAP variables. (a) Spatial position and acceleration before LC. (b) Flow and speed consistency. (c) Flow and curve direction between 800–1600 m. (d) Flow and deceleration lane length. (e) Flow and ramp type. (f) 800–1600 m curve direction in front of the diversion zone and ramp type.

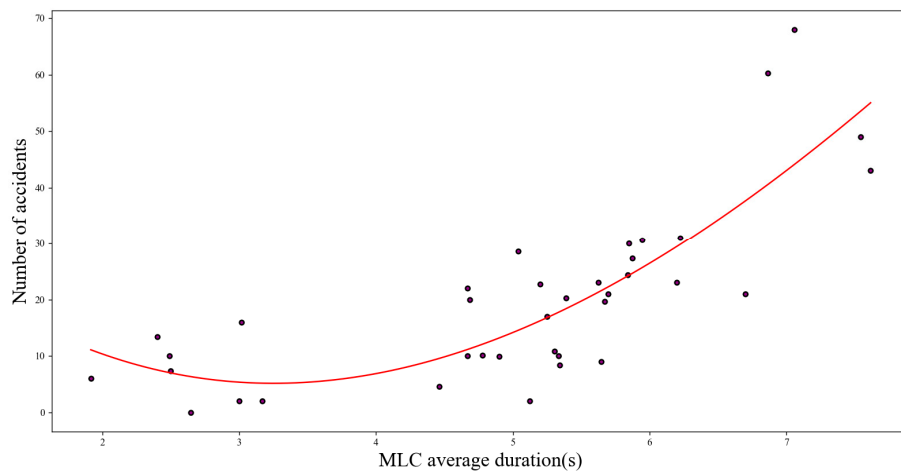


**Figure 11.** Scatter plot of the average duration of MLCs at interchanges and traffic accidents.

**Table 3.** The coefficients of the Cox-pH model (with and without frailty).

Cox PH with Frailty (Gamma Distribution)	Cox PH without Frailty
$x_2$	0.001
$x_3$	0.299
$x_5$	-0.858
$x_6$	-0.440
$x_7$	-0.003
$x_8$	-0.761
$x_9$	0.500
$x_{11}$	1.348
$x_{12}$	-2.099
$x_{13}$	-0.217

#### 4.6. Model Evaluation and Comparison Results

We chose the consistency index, partial AIC, and logarithmic likelihood ratio test to evaluate the model. The consistency index is usually between 0 and 1, where 1 represents complete consistency and 0.5 represents random guessing. The higher the consistency index, the better the model can distinguish the survival period. Partial AIC is used to compare the effects of adding or removing variables in Cox models, and a decrease in partial AIC indicates that the fit of the model is improved by adding or removing variables. The log likelihood ratio test is used to compare two nested models. If the  $p$ -value of the log likelihood ratio test is small, the null hypothesis can be rejected, indicating significant differences between the models and the added or removed variables having an impact on the model fitting. As shown in Table 4, there are some differences between the standard Cox PH model and the improved model. Specifically, the factor indicators in the time-varying Cox model using GAM technology are higher than those in the standard model, with a consistency index of 0.85 and a log likelihood ratio test of 196.20. In the standard Cox model, the consistency index is 0.8 and the log likelihood ratio test is 377.15. Unlike this result, after adding the shared fragility parameter, the consistency index of the two models increased to 0.9, but the logarithmic likelihood ratio test increased to 964.63. The improvement of the consistency index indicates that the model's ability to rank or distinguish individual risks is enhanced, which means that the prediction accuracy of the model in practical applications is improved, although the decrease in the logarithmic likelihood ratio test reflects some of the risk of overfitting. In addition, there were 17 important variables in the models before and after adding shared fragility, and the fragility period was significant ( $p$ -value < 0.001). Therefore, the fragility shared by the drivers improves the

accuracy of the Cox model. However, if only the shared fragility of the interchanges is increased, all variables related to road geometry design are excluded, that is, the driver's MLC on any interchange is related to the spatial location, nighttime speed, traffic flow time variables, and the acceleration of its own state. After excluding variables, the consistency index (0.77) significantly decreased, as shown in Table 4. In addition, if both the random effects of the drivers and road segments are considered, the model is only related to spatial position and acceleration. This also indicates that the Cox model introduces the randomness of drivers to capture the variability of unconsidered explanatory data and emphasizes the important impact of road geometry design on MLC behavior.

**Table 4.** Comparison of other Cox-related models.

	Concordance	Partial AIC	Log-Likelihood Ratio Test
Standard model	0.80	2628.94	337.15
GAM-Cox model	0.84	2452.53	228.77
GAM-Time-Varying Cox model	0.85	2114.23	196.20
Add driver random effects (Gamma)	0.90	5750.66	964.63
Add driver random effects (Weibull)	0.90	5726.56	942.46
Add random effects of interchanges	0.77	3678.85	249.63
Random effects of drivers and interchanges	0.76	2034.59	132.99
AFT	0.79	3654.20	521.42

In addition, due to the widespread application of AFT models in lane changing modeling, we compared the standard AFT model with the Cox model. Unlike Cox, the AFT model assumes that covariates have an accelerating or slowing effect on survival time and survival time follows a specific distribution. As shown in Table 4, the evaluation of the AFT model is lower than that of the standard Cox model. We determined that the AFT model made assumptions about the distribution of survival time (Weibull distribution). The advantage of this assumption is that it can directly model the duration of FLC on general road sections, but the actual data of MLCs in interchange areas may not fully conform to these distributions. However, the Cox model did not make specific assumptions about the distribution of the MLCD and can be extended to consider the temporal dependence of variables, making it more suitable for modeling MLCD in complex interchange scenarios.

Next, we use a shared fragility multiplier with Weibull distribution to correct the Cox PH model. There is almost no difference between the shared fragility models of gamma and Weibull distributions. The concordance of the goodness of fit measurement is 0.90 and the log likelihood ratio test is 942.46. There are 17 significant variables that are similar to the results of the shared fragility model of the gamma distribution, but there is a slight difference in the risk ratio. Overall, this sensitivity analysis indicates that these findings are stable for distribution types.

## 5. Discussion

### 5.1. Main Findings and Theoretical Significance

In order to analyze the intrinsic safety of heavy trucks operating at interchanges, we used large-scale, full time-domain, and high-precision floating freight vehicle data to analyze the mandatory lane changing behaviors of the main line in front of the interchange diversion area. We found that the MLCD for heavy-duty trucks is 0.5~1 s shorter than FLC, and the variance of MLCD is higher. Compared with the MLCD of small cars previously studied, heavy-duty trucks take about 0.6 s longer than small cars. Interestingly, invalid MLCDs are concentrated within 5 s, which is about 3 s longer than valid MLCs. From the position of changing lanes, MLCs are mainly distributed around 170 m to 800 m in front of the diversion zone. In addition, the relationship between accident frequency and MLCD

shows a concave curve, with fewer accidents occurring within an average lane changing time of 5 s. However, the growth rate of accidents sharply increased after 5 s, indicating that the longer the exposure time for lane changing, the more likely it is to lead to high-frequency accidents. The model we have established indicates that the distance of vehicles reaching the diversion point, consistency in geometric design, traffic volume, day and night, direction of bending of a circular curve, ramp type, length of deceleration lane, radius of road circular curve, and number of deceleration lanes have a significant impact on the risk of heavy truck MLCs, and the degree of these effects can be expressed by the relative risk value of the model. Importantly, these impacts are nonlinear and have diurnal differences. In addition, the SHAP tool indicates that there are complex interactions among various factors, among which the consistency index of operating speed, the direction of bending of a circular curve, and ramp type under different traffic volumes have varying degrees of impact on the duration of MLCs. This difference is also reflected in the relationship between the distance and speed of vehicles reaching the diversion point, as well as the relationship between the direction of bending of a circular curve and the type of ramp and the length of the deceleration lane.

We provide a full time-domain trajectory big data-driven MLCD model for heavy-duty trucks at interchanges. We hope to provide a theoretical basis for improving the consistency between the design of interchanges and the lane changing characteristics of heavy-duty trucks fundamentally. We improved the standard Cox model by first using the GAM to represent the relationship between covariates and MLCD as a nonlinear risk function. The AIC index indicates that the cubic spline curve is optimal in reflecting the nonlinear characteristics of the geometric elements of interchanges. In addition, we added a time-related module to analyze the time effects of covariates, and the standard deviation of the coefficients of these covariates reflects the diurnal differences in the impact of covariates. Among them, the number of deceleration lanes and the consistency index of operating speed have a significant difference between day and night in the impact on MLCs, while the impact of the remaining elements remains basically unchanged at different time periods. In addition, we also modify the model by sharing fragility parameters to consider the heterogeneity of lane changing among different drivers. In summary, we used a time-varying Cox model with combined GAM techniques, with a consistency index of 0.90 and a log likelihood ratio test of 964.63. This has a higher consistency index than the standard model, indicating a significant enhancement in the model's ability to rank or distinguish individual risks. This means that the prediction accuracy of the model has been improved in practical applications, although the decrease in the logarithmic likelihood ratio test reflects some overfitting risks.

## 5.2. Practical Significance

Understanding the effective probability of MLCs in interchange areas and the factors influencing these events are important focus areas of concern for researchers and practitioners, as ineffective lane changes have caused a large number of serious traffic accidents in interchange areas. The feature set of important factors used in our model is now relatively easy to obtain and is usually more accurate in most interchange areas. Our research findings focus on heavy-duty trucks and consider the most adverse effects of various factors on MLCs. We hope that this probability assessment will improve the quality of road geometry design. However, the provisions on the length of deceleration lanes in the Chinese Interchange Design Guidelines are only based on considerations of the operating speed of small vehicles. However, the data suggest that this consideration may not necessarily reduce the risk of MLCs. When the direction of the curve is on the inside, the risk of a MLC in a 35–70 m-long deceleration lane is lower; when the bending direction of the curve is on the outside, the risk of a MLC is lower for deceleration lanes with a length greater than 80 m. The degree of influence of geometric elements on different traffic volumes varies. In summary, our research provides insights into the combinatorial and diverse aspects of geometric design, emphasizing the importance of considering MLCs. In

addition, with the advancement of research on autonomous vehicles, the development trend of linear design optimization has gradually changed to multi-objective optimization, and the optimization goal has transitioned from economic cost to safety and ecological cost. In the interchange area, the research results and methods of this article can guide the reduction of the risk of lane changing events through reasonable design, thereby reducing energy consumption and improving overall transportation efficiency, such as optimizing the management and scheduling efficiency of autonomous driving fleets. In addition, the method proposed in this paper can reduce the lane change demand of autonomous vehicles in these areas, reduce accident risk, and improve traffic smoothness.

Ultimately, it is worth pointing out the limitations of our research. Although our data have a wide range and full time characteristics, they have a lower sampling frequency compared to NGSIM and highD. In addition, we did not consider factors such as the location of traffic signs, driver-specific factors, and differences in traffic conditions around specific MLCs. Although this has little impact on the study of variables such as geometric design, it can be considered to improve the accuracy of the model in the future. In addition, we also lack a comparison of the MLC behavior of small cars under the same interchange conditions. In the future, we will collect more high-frequency floating vehicle data on interchange types to analyze MLC characteristics under more factors.

## 6. Conclusions

This article provides a comprehensive analysis of MLCD in the diversion area of interchanges from the perspective of a survival analysis. We extracted the mandatory lane changing trajectories of 38 interchange diversion areas from the floating freight vehicle dataset in China. These trajectories were collected by the onboard GPS of heavy-duty trucks and have the characteristics of full time-domain and large scale. We improved the survival analysis model and investigated the influencing factors of MLCD, as well as the nonlinear, temporal, and interactive effects of these factors. In this comprehensive analysis, we have made some new findings and discussed the significance of modeling for safety analysis of interchange areas. We provide insights into the refined design of interchanges that consider lane changing behavior. We hope that these findings and methods will help improve our safety in interchange areas and further understand the relationship between MLCs and road geometry design.

**Author Contributions:** Conceptualization, M.Z. and Y.N.; methodology, Y.N.; software, Y.N.; validation, M.Z., C.Z., and Y.N.; formal analysis, M.Z.; investigation, Y.N.; resources, M.Z.; data curation, Y.N.; writing—original draft preparation, Y.N.; writing—review and editing, Y.N.; visualization, S.X.; supervision, B.W.; project administration, C.Z.; funding acquisition, C.Z.; funding acquisition. All authors have read and agreed to the published version of the manuscript.

**Funding:** This work was supported by the National Key Research & Development Program of China [Grant Number 2020YFC1512003]; the Sichuan Science and Technology Program [Grant Number NO:2022YFG0048]; the Science and Technology Project of Sichuan Transportation Department [Grant Number 2022-ZL-04]; the Key Research and Development Program of Shanxi Province [Grant Number No. 2021020201014].

**Institutional Review Board Statement:** Not applicable.

**Informed Consent Statement:** Not applicable.

**Data Availability Statement:** The data presented in this study are available on request from the corresponding author.

**Conflicts of Interest:** The authors declare no conflict of interest.

## References

- Ali, Y.; Haque, M.M.; Zheng, Z.; Washington, S.; Yildirimoglu, M. A hazard-based duration model to quantify the impact of connected driving environment on safety during mandatory lane-changing. *Transp. Res. Part C-Emerg. Technol.* **2019**, *106*, 113–131. <https://doi.org/10.1016/j.trc.2019.07.015>.

2. Venthuruthiyil, S.P.; Chunchu, M. Interrupted and uninterrupted lane changes: A microscopic outlook of lane-changing dynamics. *Transp. A-Transp. Sci.* **2022**, *18*, 1679–1698. <https://doi.org/10.1080/23249935.2021.1965240>.
3. Ali, Y.; Haque, M.M.; Zheng, Z. An Extreme Value Theory approach to estimate crash risk during mandatory lane-changing in a connected environment. *Anal. Methods Accid. Res.* **2022**, *33*, 100193. <https://doi.org/10.1016/j.amar.2021.100193>.
4. Kusuma, A.; Liu, R.; Choudhury, C. Modelling lane-changing mechanisms on motorway weaving sections. *Transp. B-Transp. Dyn.* **2020**, *8*, 1–21. <https://doi.org/10.1080/21680566.2019.1703840>.
5. Lv, W.; Xu, J.; Gao, C. A rollover safety margin-based approach for quantifying the tractor-semitrailers' emergency lane-changing response on expressway curves. *PLoS ONE* **2023**, *18*, e0291783. <https://doi.org/10.1371/journal.pone.0291783>.
6. Zhou, X.; Pan, B.; Shao, Y. Evaluating the Impact of Sight Distance and Geometric Alignment on Driver Performance in Freeway Exits Diverging Area Based on Simulated Driving Data. *Sustainability* **2021**, *13*, 6368. <https://doi.org/10.3390/su13116368>.
7. De Almeida, R.T.; Pimentel Vasconcelos, A.L.; Cesar Bastos Silva, A.M. Design consistency index for two-lane roads based on continuous speed profiles. *Promet-Traffic Transp.* **2018**, *30*, 231–239.
8. Anitha, J.; Jisha, A.; Mohan, R.M. Development of Consistency Evaluation Criteria for Indian Two-Lane Rural Highways. *Transp. Res.* **2020**, *45*, 567–577. [https://doi.org/10.1007/978-981-32-9042-6\\_45](https://doi.org/10.1007/978-981-32-9042-6_45).
9. Zhou, H.; Toth, C.; Guensler, R.; Laval, J. Hybrid modeling of lane changes near freeway diverges. *Transp. Res. Part B-Methodol.* **2022**, *165*, 1–14. <https://doi.org/10.1016/j.trb.2022.09.002>.
10. Xu, L.; Guo, C. CoxNAM: An interpretable deep survival analysis model. *Expert Syst. Appl.* **2023**, *227*, 120218. <https://doi.org/10.1016/j.eswa.2023.120218>.
11. Coupe, C. Modeling Linguistic Variables with Regression Models: Addressing Non-Gaussian Distributions, Non-independent Observations, and Non-linear Predictors with Random Effects and Generalized Additive Models for Location, Scale, and Shape. *Front. Psychol.* **2018**, *9*, 513. <https://doi.org/10.3389/fpsyg.2018.00513>.
12. Zhang, Z.; Reinikainen, J.; Adeleke, K.A.; Pieterse, M.E.; Groothuis-Oudshoorn, C.G.M. Time-varying covariates and coefficients in Cox regression models. *Ann. Transl. Med.* **2018**, *6*, 121. <https://doi.org/10.21037/atm.2018.02.12>.
13. Ali, Y.; Zheng, Z.; Haque, M.M. Modelling lane-changing execution behaviour in a connected environment: A grouped random parameters with heterogeneity-in-means approach. *Commun. Transp. Res.* **2021**, *1*, 100009. <https://doi.org/10.1016/j.commtr.2021.100009>.
14. Woo, H.; Sugimoto, M.; Madokoro, H.; Sato, K.; Tamura, Y.; Yamashita, A.; Asama, H. Goal Estimation of Mandatory Lane Changes Based on Interaction between Drivers. *Appl. Sci.* **2020**, *10*, 3289. <https://doi.org/10.3390/app10093289>.
15. Yuan, J.; Abdel-Aty, M.; Cai, Q.; Lee, J. Investigating drivers' mandatory lane change behavior on the weaving section of freeway with managed lanes: A driving simulator study. *Transp. Res. Part F-Traffic Psychol. Behav.* **2019**, *62*, 11–32. <https://doi.org/10.1016/j.trf.2018.12.007>.
16. Gong, S.; Du, L. Optimal location of advance warning for mandatory lane change near a two-lane highway off-ramp. *Transp. Res. Part B-Methodol.* **2016**, *84*, 1–30. <https://doi.org/10.1016/j.trb.2015.12.001>.
17. Lee, T.; Choi, Y.-Y.; Kho, S.-Y.; Kim, D.-K. Multilevel model for ramp crash frequency that reflects heterogeneity among ramp types. *Ksce J. Civ. Eng.* **2018**, *22*, 311–319. <https://doi.org/10.1007/s12205-017-1994-7>.
18. Cao, P.; Hu, Y.; Miwa, T.; Wakita, Y.; Morikawa, T.; Liu, X. An optimal mandatory lane change decision model for autonomous vehicles in urban arterials. *J. Intell. Transp. Syst.* **2017**, *21*, 271–284. <https://doi.org/10.1080/15472450.2017.1315805>.
19. Sharma, S.; Snelder, M.; Tavasszy, L.; van Lint, H. Categorizing Merging and Diverging Strategies of Truck Drivers at Motorway Ramps and Weaving Sections using a Trajectory Dataset. *Transp. Res. Rec.* **2020**, *2674*, 855–866. <https://doi.org/10.1177/0361198120932568>.
20. Li, Y.; Li, L.; Ni, D. Comparative Univariate and Regression Survival Analysis of Lane-Changing Duration Characteristic for Heavy Vehicles and Passenger Cars. *J. Transp. Eng. Part A-Syst.* **2022**, *148*, 04022109. <https://doi.org/10.1061/JTEPBS.0000771>.
21. Li, Y.; Li, L.; Ni, D.; Zhang, Y. Comprehensive survival analysis of lane-changing duration. *Measurement* **2021**, *182*, 109707. <https://doi.org/10.1016/j.measurement.2021.109707>.
22. Feng, Y.; Yan, X. Support Vector Machine Based Lane-Changing Behavior Recognition and Lateral Trajectory Prediction. *Comput. Intell. Neurosci.* **2022**, *2022*, 3632333. <https://doi.org/10.1155/2022/3632333>.
23. Ali, Y.; Zheng, Z.; Haque, M.M. Connectivity's impact on mandatory lane-changing behaviour: Evidences from a driving simulator study. *Transp. Res. Part C Emerg. Technol.* **2018**, *93*, 292–309. <https://doi.org/10.1016/j.trc.2018.06.008>.
24. Shang, T.; Lian, G.; Zhao, Y.; Liu, X.; Wang, W. Off-Ramp Vehicle Mandatory Lane-Changing Duration in Small Spacing Section of Tunnel-Interchange Section Based on Survival Analysis. *J. Adv. Transp.* **2022**, *2022*, 9427052. <https://doi.org/10.1155/2022/9427052>.
25. Jokhio, S.; Olleja, P.; Baergman, J.; Yan, F.; Baumann, M. Analysis of Time-to-Lane-Change-Initiation Using Realistic Driving Data. *IEEE Trans. Intell. Transp. Syst.* **2023**, *25*, 4620–4633. <https://doi.org/10.1109/TITS.2023.3329690>.
26. Dillmann, J.; den Hartigh, R.J.R.; Kurpiers, C.M.; Pelzer, J.; Raisch, F.K.; Cox, R.F.A.; de Waard, D. Keeping the driver in the loop through semi-automated or manual lane changes in conditionally automated driving. *Accid. Anal. Prev.* **2021**, *162*, 106397. <https://doi.org/10.1016/j.aap.2021.106397>.
27. Ji, A.; Ramezani, M.; Levinson, D. Joint modelling of longitudinal and lateral dynamics in lane-changing maneuvers. *Transp. B-Transp. Dyn.* **2023**, *11*, 996–1025. <https://doi.org/10.1080/21680566.2022.2154717>.
28. Li, Z.; Zhao, X. Buckley-James estimation of generalized additive accelerated lifetime model with ultrahigh-dimensional data. *Stat. Anal. Data Min.* **2023**, *16*, 305–312. <https://doi.org/10.1002/sam.11615>.

29. Ben-Assuli, O.; Ramon-Gonen, R.; Heart, T.; Jacobi, A.; Klempfner, R. Utilizing shared frailty with the Cox proportional hazards regression: Post discharge survival analysis of CHF patients. *J. Biomed. Inform.* **2023**, *140*, 104340. <https://doi.org/10.1016/j.jbi.2023.104340>.
30. Mardhiah, K.; Wan-Arfah, N.; Naing, N.N.; Hassan, M.; Chan, H.-K. Comparison of Cox proportional hazards model, Cox proportional hazards with time-varying coefficients model, and lognormal accelerated failure time model: Application in time to event analysis of melioidosis patients. *Asian Pac. J. Trop. Med.* **2022**, *15*, 128–134. <https://doi.org/10.4103/1995-7645.340568>.
31. Parsa, A.B.; Movahedi, A.; Taghipour, H.; Derrible, S.; Mohammadian, A. (Kouros) Toward safer highways, application of XGBoost and SHAP for real-time accident detection and feature analysis. *Accid. Anal. Prev.* **2020**, *136*, 105405. <https://doi.org/10.1016/j.aap.2019.105405>.
32. Puphal, T.; Flade, B.; Probst, M.; Willert, V.; Adamy, J.; Eggert, J. Online and Predictive Warning System for Forced Lane Changes Using Risk Maps. *IEEE Trans. Intell. Veh.* **2022**, *7*, 616–626. <https://doi.org/10.1109/TIV.2021.3091188>.
33. Chauhan, P.; Kanagaraj, V.; Asaithambi, G. Understanding the mechanism of lane changing process and dynamics using microscopic traffic data. *Phys. A-Stat. Mech. Its Appl.* **2022**, *593*, 126981. <https://doi.org/10.1016/j.physa.2022.126981>.
34. Luo, Q.; Zang, X.; Cai, X.; Gong, H.; Yuan, J.; Yang, J. Vehicle Lane-Changing Safety Pre-Warning Model under the Environment of the Vehicle Networking. *Sustainability* **2021**, *13*, 5146. <https://doi.org/10.3390/su13095146>.

**Disclaimer/Publisher's Note:** The statements, opinions and data contained in all publications are solely those of the individual author(s) and contributor(s) and not of MDPI and/or the editor(s). MDPI and/or the editor(s) disclaim responsibility for any injury to people or property resulting from any ideas, methods, instructions or products referred to in the content.